Journal of Materials Processing Technology 214 (2014) 2537–2544

Contents lists available at ScienceDirect

Journal of Materials Processing Technology

journal homepage: www.elsevier.com/locate/jmatprotec

Batch-mode micropatterning of carbon nanotube forests using UV-LIGA assisted micro-electro-discharge machining

Mirza Saquib us Sarwar, Masoud Dahmardeh, Alireza Nojeh*, Kenichi Takahata**

Department of Electrical and Computer Engineering, University of British Columbia, 2332 Main Mall, Vancouver, BC V6T 1Z4, Canada

ARTICLE INFO

Article history:
Received 24 February 2014
Accepted 5 May 2014
Available online 13 May 2014

Keywords:
Carbon nanotube forests
Micro-electro-discharge machining
Batch-mode micropatterning
Electrode arrays
UV-LIGA process

ABSTRACT

This paper reports batch-mode, three-dimensional micropatterning for arrays of vertically aligned carbon nanotubes, also known as CNT forests, based on dry micro-electro-discharge machining (μEDM). The process employs an array of copper electrodes microfabricated through an advanced UV-LIGA process enabled with a new photoresist system in combination with electroplating, providing a low-cost path to constructing high-density arrays of μEDM electrodes for high-throughput parallel processing. The fabricated arrays of 85-μm-tall electrodes are utilized to demonstrate and characterize planar dry μEDM for post-growth patterning of CNT forests in air. Die sinking and scanning processes are tested to show pattern transfers with a 4-μm tolerance and an average surface roughness of 230 nm. An elemental analysis suggests that contamination of the electrode material on the produced patterns is minimal. Key characteristics in the use of planar electrodes for batch processing of CNT forests are revealed through experimental analysis and discussed in detail. The results suggest that the investigated process is a promising approach toward offering a cost-effective manufacturing technology for future products functionalized with custom-designed microstructures of CNT forests.

1. Introduction

Vertically aligned carbon nanotubes, so called CNT forests, are being considered as a promising functional bulk material for forthcoming micro-electro-mechanical systems (MEMS) and various other applications owing to their unique electrical, mechanical, thermal, and other properties as discussed by Rakov (2013). CNT forests are grown using the chemical vapor deposition (CVD) process, in which the nanotubes are self-aligned due to crowding at the beginning of their growth; Verploegen et al. (2011) has provided valuable insights in their characterization of the CNT forest. This attracting material enables a broad range of potential applications, including field-emission sources demonstrated by Heer et al. (1995), sensors by Li et al. (2003), electrical interconnects by Wang et al. (2011), heat sinks by Fu et al. (2012), biomimetic adhesives by Hu et al. (2013), and scanning probes by Xiao et al. (2013). Locally selective growth of CNT forests can be performed through a typical CVD process with pre-patterned catalyst as shown by Sohn et al. (2001). However, these patterned structures are limited to two-dimensional geometries with uniform height. To expand the applications of this material into new frontiers, it is essential to establish a technique to create free-form, three-dimensional (3D) structures from post-growth forests. Micropatterning of arbitrary 3D microstructures with high-aspect ratios in CNT forests has been demonstrated by Khalid et al. (2010) using a process based on micro-electro-discharge machining (μEDM). Pyramid-like microstructures in CNT forests have been machined with this process by Dahmardeh et al. (2011), which may enable geometric enhancement of field emission from the material as shown by Zhao et al. (2011). Xiao et al. (2013) developed an advanced scanning probe for atomic force microscopy (AFM) by creating needle-like conical structures of CNT forest on silicon cantilevers using the process. These are among the extensive prospects that rely on the ability to micropattern 3D structures with varying heights and angled surfaces in the material.

μEDM is a technique for micromachining any electrically conductive solid-state material. The process utilizes pulses of thermo-mechanical impact induced by a miniaturized electrical discharge generated between a microscopic electrode and a workpiece, and is typically performed in dielectric liquid. The miniaturized arc discharge locally melts and evaporates the material at the arc spot, and micromachining is performed by repeating the unit removal by a single pulse at high frequencies while controlling the relative position between the electrode and the workpiece

* Corresponding author. Tel.: +1 604 827 4346.
** Corresponding author. Tel.: +1 604 827 4241.
E-mail addresses: anojeh@ece.ubc.ca (A. Nojeh), takahata@ece.ubc.ca (K. Takahata).

http://dx.doi.org/10.1016/j.jmatprotec.2014.05.007
0924-0136/

as explained by Masaki et al. (1990). In the case of CNT forests being the workpiece of the process, the dielectric liquid is replaced by air since the liquid tends to alter the vertical orientation of the nanotubes upon evaporation, owing to capillary forces as discussed by Dahmardeh et al. (2011). Dahmardeh et al. (2011) also reported that the removal mechanism in this dry μEDM of CNT forests was fundamentally different from that in the conventional wet process; the removal of CNTs was associated with local oxygen plasma etching thermally induced by generated pulses of arc discharge, rather than direct melting/evaporation of the material. The electrodes used were conventional cylindrical tungsten with diameters ranging from a few 10's μm to 300 μm. Although dry-μEDM patterning of the forests was shown to provide high precision in the removal process with submicron tolerance, one essential issue in light of its application for product manufacturing is low throughput due to the serial nature of the technology. In addition, since the microstructures are produced individually, dimensional accuracy in the machined structures due to the consumption of the electrode itself and/or the adhesion of removed material or debris on the electrode, is a potential concern as suggested by Saleh et al. (2013).

This study is aimed at exploring batch-mode micropatterning of CNT forests using planar electrode arrays, in order to overcome the impediments involved in dry μEDM of the material. Parallel μEDM that uses arrays of high-aspect-ratio electrodes was reported for wet processing of metals by Takahata and Gianchandani (2002). The arrays of electrodes in that case were fabricated using LIGA technology. LIGA uses deep X-ray lithography to generate high-aspect-ratio micro molds and replicate the shapes of the molds into metal structures using an electroplating process as discussed by Guckel (1998). Arrays of these electroplated microstructures were demonstrated to effectively work as μEDM electrodes by Takahata and Gianchandani (2002), enabling parallel micromachining of bulk metals in dielectric oil with >100× throughput over conventional serial μEDM. X-ray lithography requires the use of synchrotron sources whose availability is significantly limited and renders the process to be costly and thus incongruous with commercial implementation. This paper is focused on two main objectives: (1) the development of arrayed μEDM electrodes of copper fabricated through standard ultraviolet (UV) photolithography enabled with a chemically amplified, thick photoresist system, and (2) characterization of batch-mode dry μEDM of CNT forests, using the fabricated arrays of copper electrodes. The parallel processing approach to micropatterning of CNT forests is expected to open a novel path to high-throughput production of different types of advanced devices enabled with 3D-patterned structures of the material. Moreover, the use of optical lithography in combination with electroplating, known as UV-LIGA (the process concept is discussed by Chang and Kim (2000)), will make the fabrication of arrayed μEDM electrode devices compatible with typical integrated-circuit microfabrication facilities, hence significantly improving the applicability and cost effectiveness of the approach.

2. Experimental set-up and preparation

The schematic in Fig. 1a illustrates the micropatterning experiments. The set-up is based on a commercial μEDM system (EM203, Smaltec International Inc., IL, USA) that employs a relaxation-type (resistor-capacitor, or *RC*) pulse generator powered by a variable DC voltage source. In this type of pulse generation circuit, the discharge energy of a single pulse that determines a unit removal in the process can be expressed as $CV^2/2$, where C is the total capacitance of the *RC* pulse generation circuit, and V is the applied voltage. The numerical ranges of theses circuit parameters used in the experiments are also shown in the figure. The system has servo-controlled 3-axis stages with a 100-nm positioning resolution, comprised of the XY stage with the metallic holder on which the workpiece, a CNT forest on the substrate, is held and the Z stage to position the lithographically fabricated electrode array vertically. The Z stage is configured to have a planar sample holder made of ceramics, on which the electrode substrate is fixed and electrically coupled with the discharge circuit using conductive adhesive tape as depicted in Fig. 1a. The image in Fig. 1b shows the actual system. The current pulses generated are monitored using an inductive current probe (CT-1, Tektronix Inc., OR, USA) coupled with the discharge circuit and connected to an oscilloscope; readouts of the current signals are obtained via a GPIB interface connected to a computer (Fig. 1a).

Dry μEDM processes with this setting are performed in air, in the die-sinking mode by feeding the electrode array using the Z stage into the CNT forest, partly with horizontal scanning of the forest using the XY stage with respect to the array for lateral removal of the material using the array. As will be described in the subsequent section, the electrode arrays are fabricated on the silicon substrate via copper electroplating to attain a height of up to 85 μm so that deep patterning for depths of 70 μm or greater can be tested. These electrodes are defined as the cathode whereas the CNT forest is connected as the anode in the circuit (as shown in Fig. 1a).

The CNT forests utilized in this study were grown on silicon substrates with iron catalyst by means of an ethylene-based atmospheric-pressure CVD process. Details of the CVD process used for the forest growth is similar to the work of Saleh et al. (2011). The forests of multi-walled CNTs with heights of a few 100's μm grown on highly doped *n*-type silicon substrates (with resistivity and thickness of 0.001–0.005 Ω cm and 525 μm, respectively) are obtained through this process and used for experiments. A piece of the forest sample is then fixed on the metallic holder on the XY stage using adhesive tape, which aids in establishing a low-resistance connection between the forest and the discharge circuit.

3. Microfabrication of electrode arrays

3.1. Materials selection

One key factor involved in the development of the arrayed electrode device is the photoresist suitable for the targeted microfabrication process. An epoxy-based photoresist called SU-8 (MicroChem Corp., MA, USA) has been widely used in UV LIGA, as it can be spin coated to form a very thick layer. As demonstrated by Lee et al. (2011), this allows for high-aspect-ratio photo-patterning owing to its mechanical properties and low optical absorption in the near UV range leading to a uniform exposure condition across the thickness; a patterning thickness of over 1000 μm (established by repeated spin coatings) with an aspect ratio of 18 was reported by Lorenz et al. (1998). Regardless of these appealing features, as shown by Chang and Kim (2000), the use of SU-8 poses an inherent difficulty in the removal of the cross-linked epoxy material, a requirement for the resist to be used as the mold for electroplating to yield free-standing electroplated structures on the substrate. Poly(methyl methacrylate), or PMMA, is another photoresist traditionally used for thick patterning but requires an UV exposure dose 10 times that of SU-8; this option is more suited for synchrotron X-ray lithography as used in typical LIGA processes. KMPR is a new chemically amplified photoresist jointly developed by MicroChem Corp. (MA, USA) and Nippon Kayaku Ltd. (Tokyo, Japan). It is a negative tone, i-line (365 nm) photoresist based on epoxy that is high contrast and can be coated to >100-μm thickness by a single spin coating step, enabling thick, high-aspect-ratio photo-patterning. A UV-exposed layer of this material can be developed in a conventional aqueous alkaline developer (such as tetramethylammonium hydroxide), leaving the cross-linked material that exhibits high

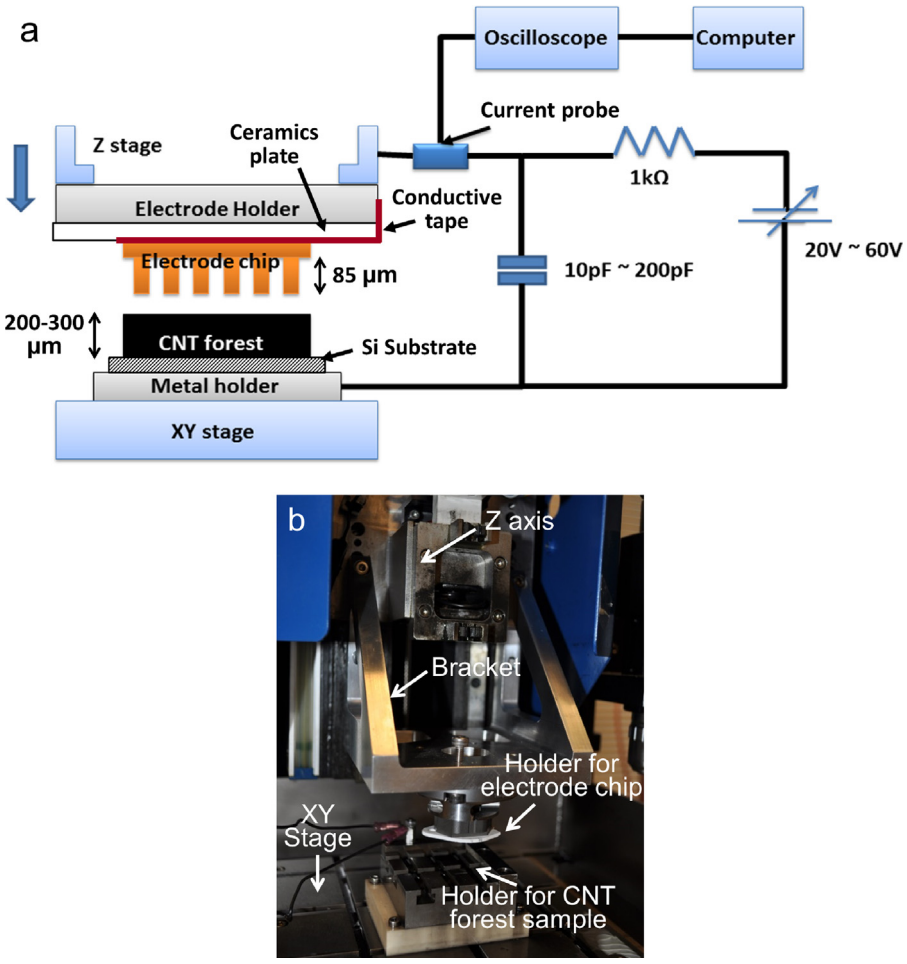

Fig. 1. Experimental set-up for batch-mode μEDM of CNT forests: (a) a schematic diagram, and (b) a photo of the apparatus.

chemical resistance, suitable for the subsequent electroplating process. One of the significant features of this photoresist is that the cross-linked material can be readily stripped using a commercial resist stripper (e.g., Remover PG). All these characteristics of KMRP make it ideal for the UV-LIGA process, including microfabrication of μEDM electrode array.

Copper is a suitable material for forming planar μEDM electrodes because high-aspect-ratio structures can be stably produced with electroplating that is compatible with lithography-based processes, while the material has high electrical and thermal conductivities, key characteristics necessary for μEDM electrodes (Jha et al. (2011) describes general performance parameters of μEDM including those of the tool electrodes). Batch-mode μEDM of alloys in dielectric oil was demonstrated by Takahata and Gianchandani (2002) using array of copper electrodes fabricated with synchrotron LIGA techniques. In light of these proven aspects, this study adopts copper to construct the electrode structures and uses them to characterize dry μEDM of CNT forests.

3.2. UV LIGA process for electrode device fabrication

An outline of the fabrication procedure for the electrode device is illustrated in Fig. 2. A wafer of the same type of heavily doped silicon is first cleaned through piranha etch, followed by oxide removal in buffered hydrofluoric acid. The wafer is then coated with a seed layer of 200-nm-thick copper together with a 20-nm-thick chromium adhesion layer by electron-beam evaporation (Fig. 2a). Next, the wafer is spin coated with an adhesion promoter (HMDS) and then the photoresist KMPR 1050 (Fig. 2b). For KMPR coating, a two-step sequence, the first with a spin speed of 500 rpm for a period of 15 s and the second with 1000 rpm for 35 s, is selected to achieve a total thickness of 90 μm (this two-step coating is found to result in higher uniformity of the final film over the wafer while reducing the waste of the resist material). Next, the wafer is soft baked on a hot plate at 100 °C for ~20 min. Immediately after this step, the surface of the photoresist layer is still in a semi-liquid state that may adhere to the optical mask used in the subsequent contact exposure. Hence, upon removal from the hot plate, the wafer is allowed to cool for the baked photoresist to set before moving to the next step. Photolithography is then performed with a UV mask aligner (Canon PLA-501F) with an i-line light source under the contact mode, using an optical mask containing the pattern of interest (Fig. 2c). UV exposure with a radiation power density of 9 mW/cm^2 for a period of 150 s is found to be an optimal condition for pattern transfer to the coated KMPR layer. Post-exposure baking is performed at 100 °C for 4 min, followed by development in an SU-8 developer solution (also suitable for KMRP development) (Fig. 2c), which leaves the cross-linked mold pattern after rinsing and drying. To ensure complete removal of the photoresist and other contaminants from the bottom of unexposed regions, imperative for the subsequent electroplating process, oxygen plasma etching is conducted after the development step. The wafer is then electroplated to grow copper structures in the recess of the photoresist mold in a sulfuric-acid-based bath (Fig. 2d). A current density of 6 mA/cm^2 is used to initiate the electroplating process and ramped up to 32 mA/cm^2 at a rate of 3 mA/cm^2 per minute; this process for a

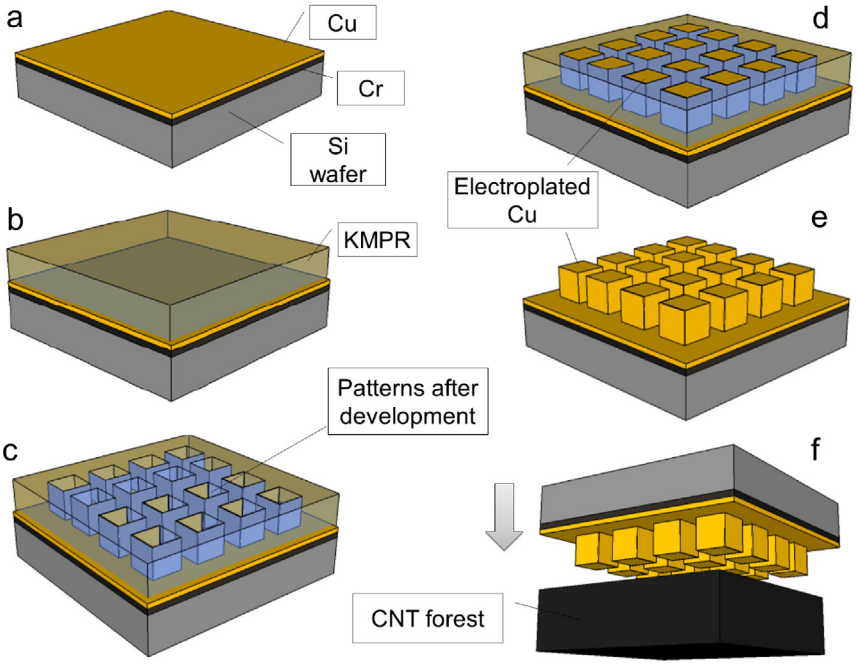

Fig. 2. Process steps for microfabrication of the electrode array and its use for planar μEDM: (a) deposit layer of copper/chromium on silicon substrate; (b) spin coat KMPR and soft bake; (c) expose and develop KMPR; (d) electroplate copper; (e) strip KMPR; (f) μEDM CNT forest using fabricated electrodes.

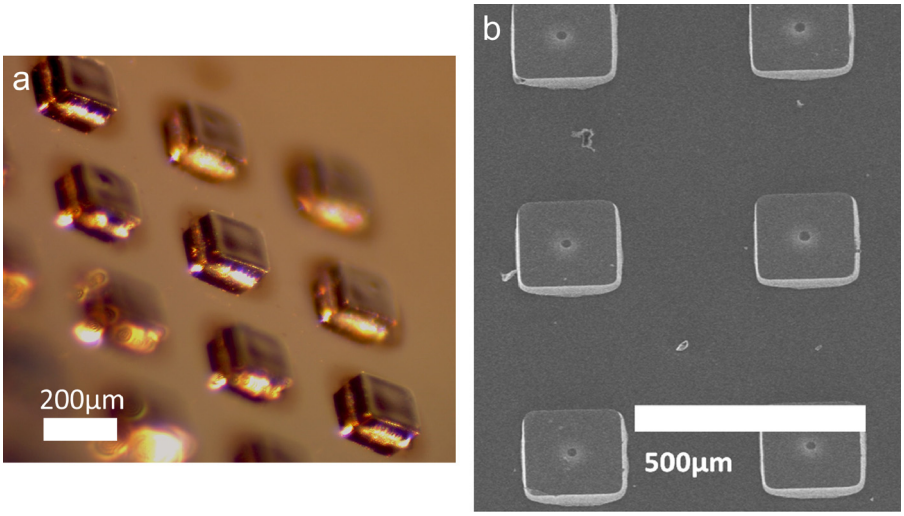

Fig. 3. (a) An optical image and (b) a scanning electron microscope (SEM) image of fabricated arrays of 85-μm-tall copper electrodes with a common 200-μm × 200-μm square pattern and 300-μm spacing.

total of 90 min produces 90-μm-tall structures. After electroplating, the KMPR mold is stripped to attain the final copper structures to be used as μEDM electrodes (Fig. 2e). The wafer is immersed in Remover PG, heated to 80 °C and agitated using a magnetic agitator, for 2–3 min; the KMPR mold expands and becomes very soft as it swells with the striper solution, losing adhesion to the substrate and eventually peeling off from it. The final device is rinsed in deionized water and dried. Fig. 2f illustrates the electrode device in use in patterning CNT forests. Fig. 3 shows images of fabricated arrays of copper electrodes with a test pattern.

3.3. Post-fabrication process

The electrode dies with selected sizes (up to 5 mm × 5 mm) are cut out from the wafer using a diamond disk saw. When each die is mounted on the *Z*-stage holder, electrical connection between the electrodes and the discharge circuit is made through the silicon substrate, with its bottom surface being electrically coupled with the circuit using conductive adhesive tape as described earlier. This electrical connection leads to a relatively high resistance between each electrode structure and the circuit, measured to be ~100 Ω, mainly due to insufficient ohmic contact with the silicon substrate. This parasitic resistance present in the circuit attenuates the discharge current in each pulse and hence the energy available for material removal, potentially limiting proper machining and/or slowing the process. In order to minimize this negative effect of the parasitic resistance, electron-beam evaporation was conducted on the electrode dies positioned at an angle to deposit thin-film copper (200-nm thickness) on the backside and sides of each die. This deposition is observed to effectively lower the resistance down to 16 Ω

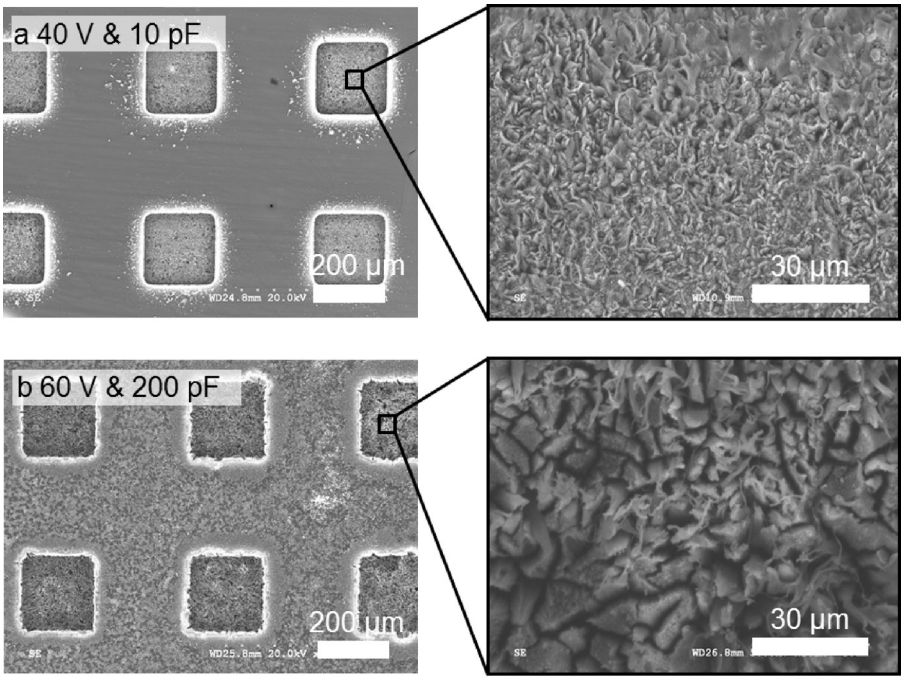

Fig. 4. Patterns of CNT forest created in the sink mode using (a) 40 V and 10 pF and (b) 60 V and 200 pF.

when the die is coupled with the circuit in the manner described above, enabling μEDM operation at low voltages yet attaining the current levels necessary to drive proper CNT removal.

4. Experimental results and discussion

The feasibility and characteristics of planar μEDM of CNT forests was evaluated using the fabricated electrode arrays with different discharge conditions in air. The patterning test was first implemented in the die-sinking mode, where the forest sample was patterned by feeding the array into it vertically using the *Z* stage. In this test, a 10 × 10 array of the electrodes shown in Fig. 3a and b was used to machine the forest for a depth of 70 μm. The machining tolerance and surface quality of the patterned structures are two key characteristics of a μEDM process, and the conditions that improve these characteristics are of interest in the targeted planar process. In light of this, the machining test was initiated from the electrical condition (20 V, 10 pF) that defined the least discharge energy necessary to perform conventional μEDM of CNTs as defined by Khalid et al. (2010); however, this condition resulted in the difficulty in establishing proper discharge pulses and thus in the removal of the CNTs. (This outcome could be due to two possible factors: One is the relatively high overall parasitic resistance (which includes the contact resistances at the forest sample and at the electrode device) present in the discharge circuit. The other is the short circuits – which were indeed detected – due to local arcing that could be exacerbated by the use of planar, non-rotating electrode (in contrast, the conventional case of a rotating cylindrical electrode easily breaks up an arcing condition). The voltage was then increased gradually while maintaining the capacitance value. This procedure revealed that 40 V was the lowest voltage level that led to stable generation of discharge pulses between the copper array and the CNT forest, enabling parallel patterning of the forest. This electrical condition defines the theoretical discharge energy to be 8 nJ.

A sample result from this patterning process is displayed in Fig. 4a. A comparison between the dimensions of the patterned structures shown in the SEM images and the known size of the electrode structures suggests that the tolerance of the process (i.e., a gap clearance between the sidewall surface of the patterned structure and that of the electrode) is approximately 4 μm. This value is less than half the level reported by Khalid et al. (2010) for the same voltage and capacitance; the tighter tolerance with this batch-mode implementation might be brought about by the fact that the electrodes are stationary (except for *Z*-direction feeding) with no rotating motion. (Note that the conventional setting of single-tip electrodes with rotation may suffer from an enlargement of the gap due to possible wobbling motions.) The discharge energy was further increased to observe its impact on the patterning quality and to compare the result with the lowest energy case. Fig. 4b shows the structures patterned with *V* and *C* of 60 V and 200 pF, respectively, in the same CNT-forest sample using the same electrode array. The machining tolerance under this condition was measured to be 6–10 μm. Using the two electrical settings mentioned above, another parallel patterning that combined lateral scanning motions with die sinking was also tested using an array of cylindrical copper electrodes with 140-μm diameter; examples of the results are shown in Fig. 5a and b. In all cases, the process was able to transfer the pattern of the electrodes (and that of scanning motion when it was present) to the CNT forest.

As can be seen from a comparison between the results in Fig. 4a and b, however, it is evident that the former case resulted in sharper edges and a finer surface morphology on the patterned structures compared with the latter case. This tendency is consistent with prior results reported by Khalid et al. (2010), i.e., the use of smaller possible energies (or voltages) contributes to suppressing the amount of discharge gap as well as that of unit removal of CNTs by a single pulse, leading to higher precision, as indicated by the difference in the machining tolerances noted above, and smoother surfaces. Comparing the SEM images, the case with the large energy appears to have caused bundling of the CNTs on the patterned surfaces, leading to rougher surfaces. These visual observations were verified using AFM. Fig. 6 shows the AFM images for the bottom surfaces of the patterns created in the forest using the two energy conditions and compares two 3D surface roughness parameters, average (Sa) and peak-valley height (Sy), obtained from the

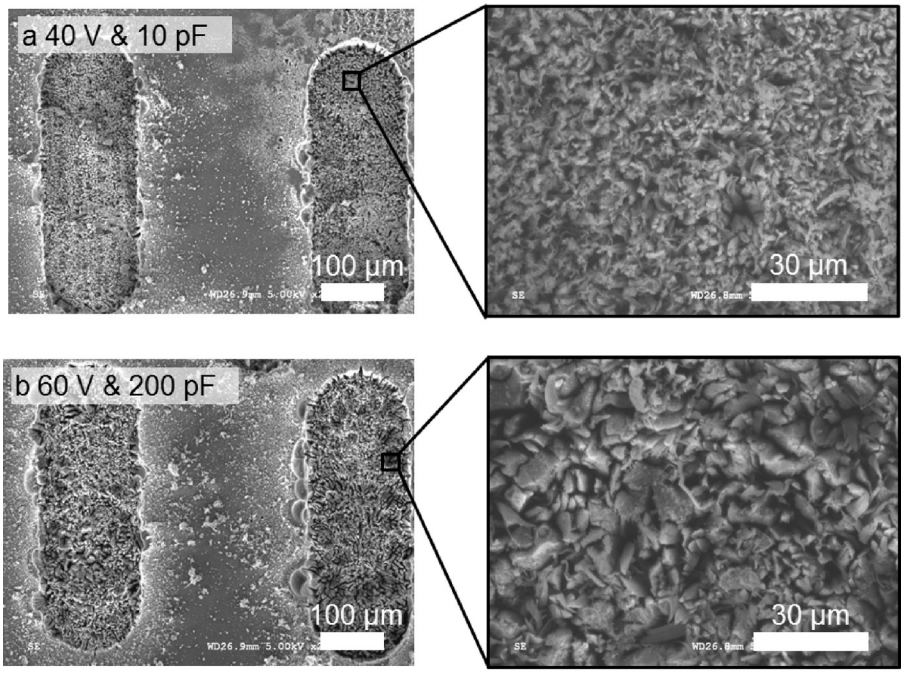

Fig. 5. Patterns of CNT forest created in the sink and scan mode using (a) 40 V and 10 pF and (b) 60 V and 200 pF.

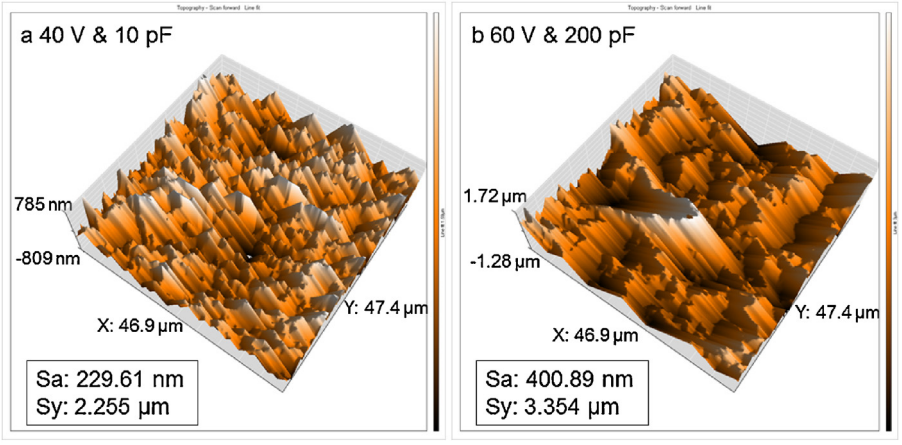

Fig. 6. AFM images of patterned regions using (a) 40 V and 20 pF and (b) 60 V and 200 pF in the sink mode. The measurement was performed with Easyscan 2 (Nanosurf AG, Liestal, Switzerland).

acquired AFM data. These comparisons indicate a degradation of surface smoothness by the use of the higher energy condition, which led to increases in Sa and Sy by 75% and 49%, respectively.

The elemental composition of the μEDMed surfaces was analyzed using energy-dispersive X-ray spectroscopy (EDX) at 20-keV beam energy. Table 1 summarizes the detected levels of the major elements involved in the patterning process and the machined materials. The result with an original (non-patterned) surface of the same forest sample is also shown in the table for comparison.

Table 1
Results from EDX elemental analysis of patterned CNT forest.

Element	Patterned area		Original surface	
	K ratio	Conc. (%)	K ratio	Conc. (%)
C	0.586	88.88	0.658	91.74
O	0.008	8.21	0.006	6.08
Si	0.021	2.63	0.017	2.17
Cu	0.002	0.27	0	0

It is observed from both the K ratio and concentration values that although copper was detected on the patterned area, its amount is very small, suggesting that the wear of the electrode due to its use for the process and the contamination on the patterned surfaces with the electrode material are negligible. This favorable condition is similar to the case of tungsten electrodes used by Saleh et al. (2012). The results also indicate that both the amount of oxygen and its change due to the process are small. The signals of silicon are presumed to originate in the silicon substrate, by detecting X-rays from it caused by impinging electrons that penetrated through the CNT forest, which consists of mostly empty space (the detection of silicon was also reported by Khalid et al. (2010)). Certain variations in the levels of carbon and silicon between the original and patterned surfaces can also be seen in Table 1. In particular, it shows that the level of carbon decreased whereas that of silicon increased after the process. These behaviors seem to be logical, as the more the amount of carbon, the less the signal received from the silicon substrate. One cause of these variations may be related to the thickness of the forest layer rather than the patterning process itself. The

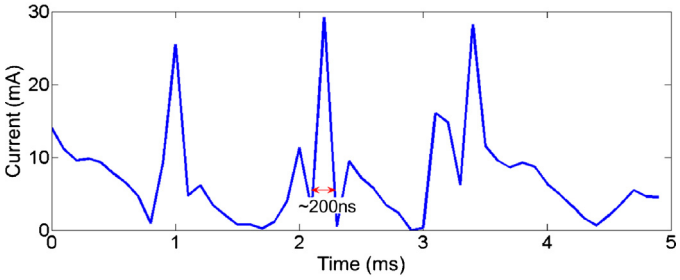

Fig. 7. A sample waveform of discharge pulses captured in the batch-mode μEDM of CNT forests.

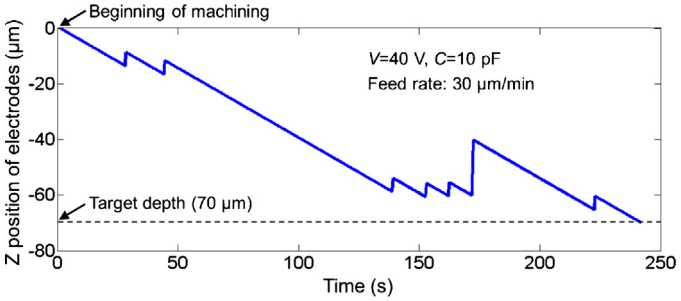

Fig. 8. The position of electrode array on the *Z* axis tracked in real time during machining.

following factors should be noted in this regard: one is that there is relatively large non-uniformity in the original height of the CNTs on a CVD-grown forest sample. Furthermore, the thickness of the forest was reduced in the patterned areas due to the removal process. These conditions could have led to a difference in the forest thickness and resultant signal level of carbon (and thus that of silicon) between the two analyzed locations. Another cause may be associated with scattering of X-ray signals from CNTs, which could occur more in the patterned area due to the surface roughness of the area (Fig. 6a) induced by the patterning process.

The average pulse current in the low energy case (40 V and 10 pF) was measured to be ~30 mA; sample current pulses captured in the process are shown in Fig. 7. This current level is comparable to those reported by Dahmardeh et al. (2011), a few to several 10's mA, for machining with similar electrical conditions (30 V, 10 pF) with the same polarity setting in air ambient. The pulse durations were recorded to be approximately 200 ns. This is 5–6× longer than those shown in the above reports. Although the exact cause of this result is not clear, it is worth considering the following conditions: The lumped capacitance and parasitic inductance of the discharge circuit are the two parameters that affect the duration as suggested by Paul et al. (2012). Both the present experiment and those discussed by Dahmardeh et al. (2011) used the same capacitance (of 10 pF), and comparing between the machining settings used in them, the levels of parasitic inductance are presumed to be similar. However, the planar electrode device used in the present study, which faces the top surface of the CNT forest in close proximity during the process (not the case in the past implementations with single-tip electrodes), can cause a parasitic capacitance much larger than that involved in the single-tip electrode case. This additional capacitance associated with the planar electrode is coupled with the external capacitor of the *RC* circuit in parallel, potentially serving as a contributing factor to the longer duration of the pulses whose energy levels could be substantially larger than the theoretical estimate.

Other possible effects particularly relevant to the use of planar electrodes for dry μEDM of CNT forests should be noted. In the setting with conventional single-tip cylindrical electrodes, the machining area was exposed to fresh ambient air, which supplied plenty of oxidation species necessary to drive local plasma etching of the nanotubes at the discharge spot as predicted by Dahmardeh et al. (2011). The circumstance is different in the batch-process setting, in which a planar electrode device maintains a micron-scale air gap with the forest sample; therefore, the access of ambient gas to the machining areas is physically limited, especially when the electrodes are fed deeper into a forest and hence the gap spacing between the electrode substrate and the forest becomes narrower. Nevertheless, the CNT forest is essentially a porous bulk material, whose 95% of the volume is occupied by air as analyzed by Esconjauregui et al. (2013), and this internal air is available for dry etching of the CNTs. These conditions related to the supply of etch species might affect the process.

The measured *Z* position of the electrode array tracked during the μEDM process performed with a feed rate setting of 30 μm/min is shown in Fig. 8. The ripples seen in the plot were caused by short-circuit events, i.e., when the system detects a short while feeding the electrodes, it automatically retracts the *Z* stage until the short condition is cleared and resumes feeding again after that point. Consequently, the occurrence of shorting slows down the process; the particular process shown in Fig. 8 completed in 240 s, representing an effective feed rate of 17.5 μm/min. As displayed in the plot, shorting occurred more frequently when the electrode approached closer to the target depth (70 μm). One possible cause behind this outcome may be associated with the non-uniformity of the forest material; as the electrode device was fed deeper, some large portion of the forest surface may have come closer to the substrate of the device, having a gap distance small enough to start generating discharge with the electrode substrate, leading to frequent short circuits. Another possibility could be related to the circumstance of the ambient gas noted above, i.e., the etch species may become depleted at the machining site as electrode feeding limits the supply of ambient air. Given the fact that μEDM of CNT forest without oxygen (or only with nitrogen) is not feasible due to frequent arcing as shown by Saleh et al. (2013), the above situation could be relevant to the observed shorting behavior.

The bundling-like effect observed on the patterned CNTs surfaces with the high-energy processing could be another unique effect related to the use of planar electrodes. The serial μEDM of CNT forests with rotating electrodes used by Dahmardeh et al. (2011) did not appear to cause this type of effect. The rotation of electrodes dissipates heat generated during the discharge process more effectively than in the case without it (the case of the batch-mode process). Bundling of CNTs due to thermal effects has been reported previously by Terrones et al. (2002). One possible measure to circumvent or mitigate the issue may be to combine vertical vibration of the sample with the machining process. The vibratory motion of μEDM electrode/workpiece is known to enhance debris flushing and smooth processing in traditional wet μEDM as reported by Zhao et al. (2004). In case of dry μEDM, the combinational use of vibration is expected to promote air flow, which may be effective in fulfilling the two potential needs discussed above, i.e., heat dissipation from and supply of etchant species to the machining regions.

5. Conclusion

A micropatterning method for vertically aligned CNT forests based on lithography-assisted dry μEDM has been studied. Planar and parallel patterning of microstructures in the nanotube material was demonstrated using arrays of copper electrodes that were microfabricated using a UV-LIGA process developed. Batch-mode

μEDM of CNT forests was experimentally shown to be feasible with the lowest discharge voltage of 40 V in the sinking mode alone and also in combination with scan mode using the arrays. The surfaces of patterned microstructures created in the forest exhibited sharp edges with an average 3D surface roughness of ~230 nm. EDX analysis revealed both negligible contamination of the electrode material and minimal consumption of the electrodes caused by the discharge process. The effects in the use of planar electrodes specific to the batch-mode processing of CNT forests were discussed along with the electrical, surface, and process characteristics observed experimentally. The developed process is potentially scalable to very large-area processing and suitable for mass production of a variety of advanced MEMS and other devices enabled by this promising material. Future work includes further optimization of the UV-LIGA process for demonstrating high-aspect-ratio electrodes with larger-scale arrays as well as 3D parallel μEDM using these electrodes with improved performance in throughput and resolution of the process.

Acknowledgments

This work was partially supported by the Natural Sciences and Engineering Research Council of Canada, the Canada Foundation for Innovation, the British Columbia Knowledge Development Fund, and the BCFRST Foundation/British Columbia Innovation Council. K. Takahata is supported by the Canada Research Chairs program.

References

Chang, H.-K., Kim, Y.-K., 2000. UV-LIGA process for high aspect ratio structure using stress barrier and C-shaped etch hole. Sens. Actuators A: Phys. 84, 342–350.

Dahmardeh, M., Nojeh, A., Takahata, K., 2011. Possible mechanism in dry micro-electro-discharge machining of carbon-nanotube forests: a study of the effect of oxygen. J. Appl. Phys. 109, 93304–93308.

Esconjauregui, S., Xie, R., Fouquet, M., Cartwright, R., Hardeman, D., Yang, J., Robertson, J., 2013. Measurement of area density of vertically aligned carbon nanotube forests by the weight-gain method. J. Appl. Phys. 113, 144309.

Fu, Y., Nabiollahi, N., Wang, T., Wang, S., Hu, Z., Carlberg, B., Zhang, Y., Wang, X., Liu, J., 2012. A complete carbon-nanotube-based on-chip cooling solution with very high heat dissipation capacity. Nanotechnology 23, 045304.

Guckel, H., 1998. High-aspect-ratio micromachining via deep X-ray lithography. Proc. IEEE 86, 1586–1593.

Heer, W.A., de Châtelain, A., Ugarte, D., 1995. A carbon nanotube field-emission electron source. Science 270, 1179–1180.

Hu, S., Xia, Z., Dai, L., 2013. Advanced gecko-foot-mimetic dry adhesives based on carbon nanotubes. Nanoscale 5, 475–486.

Jha, B., Ram, K., Rao, M., 2011. An overview of technology and research in electrode design and manufacturing in sinking electrical discharge machining. J. Eng. Sci. Technol. Rev. 4, 118–130.

Khalid, W., Ali, M.S.M., Dahmardeh, M., Choi, Y., Yaghoobi, P., Nojeh, A., Takahata, K., 2010. High-aspect-ratio, free-form patterning of carbon nanotube forests using micro-electro-discharge machining. Diam. Relat. Mater. 19, 1405–1410.

Lee, H., Lee, K., Ahn, B., Xu, J., Xu, L., Oh, K.W., 2011. A new fabrication process for uniform SU-8 thick photoresist structures by simultaneously removing edge bead and air bubbles. J. Micromech. Microeng. 21, 125006.

Li, J., Ng, H.T., Cassell, A., Fan, W., Chen, H., Ye, Q., Koehne, J., Han, J., Meyyappan, M., 2003. Carbon nanotube nanoelectrode array for ultrasensitive DNA detection. Nano Lett. 3, 597–602.

Lorenz, H., Despont, M., Fahrni, N., Brugger, J., Vettiger, P., Renaud, P., 1998. High-aspect-ratio, ultrathick, negative-tone near-UV photoresist and its applications for MEMS. Sens. Actuators A: Phys. 64, 33–39.

Masaki, T., Kawata, K., Masuzawa, T., 1990. Micro electro-discharge machining and its applications. In: IEEE Micro Electro Mechanical Systems, 1990. Proceedings, An Investigation of Micro Structures, Sensors, Actuators, Machines and Robots, pp. 21–26.

Paul, G., Roy, S., Sarkar, S., Hanumaiah, N., Mitra, S., 2012. Investigations on influence of process variables on crater dimensions in micro-EDM of γ-titanium aluminide alloy in dry and oil dielectric media. Int. J. Adv. Manuf. Technol. 65, 1009–1017.

Rakov, E.G., 2013. Materials made of carbon nanotubes. The carbon nanotube forest. Russ. Chem. Rev. 82, 538–566.

Saleh, T., Dahmardeh, M., Bsoul, A., Nojeh, A., Takahata, K., 2011. Field-emission-assisted approach to dry micro-electro-discharge machining of carbon-nanotube forests. J. Appl. Phys. 110, 103305.

Saleh, T., Dahmardeh, M., Bsoul, A., Nojeh, A., Takahata, K., 2012. High-precision dry micro-electro-discharge machining of carbon-nanotube forests with ultralow discharge energy. In: IEEE 25th International Conference on Micro Electro Mechanical Systems (MEMS), pp. 259–262.

Saleh, T., Dahmardeh, M., Nojeh, A., Takahata, K., 2013. Dry micro-electro-discharge machining of carbon-nanotube forests using sulphur-hexafluoride. Carbon 52, 288–295.

Sohn, J.I., Lee, S., Song, Y.-H., Choi, S.-Y., Cho, K.-I., Nam, K.-S., 2001. Patterned selective growth of carbon nanotubes and large field emission from vertically well-aligned carbon nanotube field emitter arrays. Appl. Phys. Lett. 78, 901–903.

Takahata, K., Gianchandani, Y.B., 2002. Batch mode micro-electro-discharge machining. J. Microelectromech. Syst. 11, 102–110.

Terrones, M., Ajayan, P.M., Banhart, F., Blase, X., Carroll, D.L., Charlier, J.C., Czerw, R., Foley, B., Grobert, N., Kamalakaran, R., Kohler-Redlich, P., Rühle, M., Seeger, T., Terrones, H., 2002. N-doping and coalescence of carbon nanotubes: synthesis and electronic properties. Appl. Phys. A: Mater. Sci. Process. 74, 355–361.

Verploegen, E., Hart, A.J., De Volder, M., Tawfick, S., Chia, K.-K., Cohen, R.E., 2011. Non-destructive characterization of structural hierarchy within aligned carbon nanotube assemblies. J. Appl. Phys. 109, 94315–94316.

Wang, T., Jeppson, K., Ye, L., Liu, J., 2011. Carbon-nanotube through-silicon via interconnects for three-dimensional integration. Small 7, 2313–2317.

Xiao, Z., Saquib Sarwar, M., Dahmardeh, M., Vahdani Moghaddam, M., Nojeh, A., Takahata, K., 2013. Cone-shaped forest of aligned carbon nanotubes: an alternative probe for scanning microscopy. Appl. Phys. Lett. 103, 171603.

Zhao, W., Wang, R.-Z., Song, X.-M., Wang, H., Wang, B., Yan, H., Chu, P.K., 2011. Electron field emission enhanced by geometric and quantum effects from nanostructured AlGaN/GaN quantum wells. Appl. Phys. Lett. 98, 152110–152113.

Zhao, Y., Zhang, X., Liu, X., Yamazaki, K., 2004. Geometric modeling of the linear motor driven electrical discharge machining (EDM) die-sinking process. Int. J. Mach. Tools Manuf. 44, 1–9.